JQSRT 1717
pp: 1-16 (col.fig.: nil)
PROD. TYPE: COM
ED: CH
PAGN: Bhanu – SCAN: Preethi

ARTICLE IN PRESS

PERGAMON

Journal of Quantitative Spectroscopy & Radiative Transfer ▮▮▮ (▮▮▮▮) ▮▮▮–▮▮▮

Journal of Quantitative Spectroscopy & Radiative Transfer

www.elsevier.com/locate/jqsrt

Half-widths of $H_2{}^{16}O$, $H_2{}^{18}O$, $H_2{}^{17}O$, $HD^{16}O$, and $D_2{}^{16}O$: I. Comparison between isotopomers

Robert R. Gamache*, Jonathan Fischer

Department of Environmental, Earth, and Atmospheric Sciences, University of Massachusetts Lowell, 1 University Avenue, Lowell, MA 01854, USA

Received 29 May 2002; accepted 3 September 2002

Abstract

Pressure-broadened half-widths are determined using the complex Robert–Bonamy (CRB) formalism for five isotopomers of water vapor. The calculations are made with nitrogen and oxygen as the perturbing gases. The intermolecular potential is taken as a sum of electrostatic contributions, Lennard-Jones (6–12) atom–atom, and isotropic induction and dispersion components. Calculations made using recently determined Lennard-Jones (L-J) parameters for deuterium are compared with previous calculations that utilized only the hydrogen L-J parameters. The dynamics of the collision process are correct to second order in time. Ratios of the half-width of the principal isotopomer to the other isotopomers are determined and discussed with particular emphasis on predicting half-widths of the lesser isotopic species from the values for the principal species.

Keywords: Half-width; $H_2{}^{16}O$; $H_2{}^{18}O$; $H_2{}^{17}O$; $HD^{16}O$; $D_2{}^{16}O$; Water vapor isotopomers

1. Introduction

The study of the Earth's climate system relies heavily on the use of remotely sensed data from satellite, balloon, and ground based instruments. The interpretation of these data requires the use of atmospheric radiative transfer (RT) models, which also are used to model natural radiative processes. In turn, these RT models need high-precision parameters describing line positions, intensities, pressure-broadened half-widths and line shifts of the gases to be studied. With time, the number of gases measured and the sensitivity of the instruments have increased steadily. This has forced the spectroscopic databases to keep pace with the needs of the remote sensing community.

* Corresponding author. Tel.: +1-978-934-3904; fax: +1-978-934-3069.
E-mail address: robert_gamache@uml.edu (R.R. Gamache).

0022-4073/02/$ - see front matter © 2002 Published by Elsevier Science Ltd.
PII: S0022-4073(02)00217-0

Of the gases in the terrestrial atmosphere, water vapor is the principle absorber of longwave radiation, responsible for some 80% of greenhouse warming of the Earth's surface [1]. In this process, water in its vapor phase plays an important and unique role, distinguishable from liquid or ice phases (clouds) in terms of spectral properties, geographic location, etc. A thorough understanding of the spectroscopy underlying the greenhouse warming, especially pressure broadening of water vapor, is important for several reasons. First, as peak absorptivity is redistributed to line wings, higher concentrations are required to saturate pressure-broadened lines. This causes an increase in the maximum radiative forcing possible, a fact that could have important consequences in radiatively unsaturated conditions such as those which prevail in the polar winter sky. A second motivation, closely related the first, derives from the fact that understanding the spectroscopy is essential to proper interpretation of remote sensing measurements of the atmosphere. Because water vapor transitions are often present in the channels used to detect and quantify other trace species, an accurate knowledge of the spectroscopic parameters of water vapor in all its isotopic variants leads to increased confidence in the quantities determined for the other trace species.

The spectral parameters for water vapor most often used for remote sensing applications are from the HITRAN [2] or GEISA [3] databases. Of these parameters, the collision-broadened half-widths and collision induced line shifts are the least well understood. The half-width data for $H_2{}^{16}O$ on the 2000 edition of the HITRAN database are a mixture of a small number of measured values (~300), a larger number of quantum Fourier transform calculations [4] (~2500), and estimated values [5]. This small data set is used for ~52 000 water vapor lines on HITRAN2000. The calculations are over 20 years old and the confidence in the measured database is also not high [6]. The data for the shift of the spectral lines are missing entirely. The data for the lesser abundant isotopomers of water vapor are those of the principal species. The effects of uncertainty in half-widths on the accuracy of retrieved parameters are well understood [7,8]. Of the parameters needed for inverting remotely sensed data, the collision-broadened half-width is the least well known for atmospheric applications [9,10]. The importance of the line shift has recently come to light [11,12].

The use of the principal species half-width data for the lesser abundant isotopomers has not been called into question since the availability of data has been limited until recently. There are now a number of measurements of the half-widths for the isotopomers of water vapor [13–18], however, the number of transitions measured is much smaller than the number of transitions on the databases. Devi et al. [13,14] made measurements of air- and N_2-broadening of ν_2 transitions for D_2O, and for HDO, $H_2{}^{16}O$ and $H_2{}^{18}O$. Rinsland et al. [15] later studied pressure broadening and pressure induced line shifts for more than 100 transitions in the ν_2 band of D_2O in air, nitrogen, and oxygen. This work was later extended [16] to consider air-, nitrogen-, and oxygen-pressure broadening and pressure induced line shifts for more than 200 transitions in the ν_2 band of $HD^{16}O$. More recently, Toth has measured a large number of air- and N_2-broadened half-widths and pressure-induced frequency shifts for transitions of HDO and D_2O from 709 to 1936 cm^{-1} [17] and $H_2{}^{16}O$, $H_2{}^{18}O$, and $H_2{}^{17}O$, from 604 to 2271 cm^{-1} [18].

In principle, theoretical calculations are an attractive alternative for determining the line shape parameters, depending upon the accuracy requirements of the radiative transfer application and the credibility of the theory. Even when laboratory measurements are available, however, certain effects (such as line mixing [19]) may still require a sophisticated theoretical model in order to unravel observed spectra. In the past, it has been difficult to gauge the theory with respect to measurement.

This situation has improved. While certainly not exhaustive, there are enough measurements to test the theoretical developments.

In this work, the half-widths are determined for a number of ground-state transitions from the HITRAN database [2] using the complex Robert-Bonamy (CRB) formalism [20]. The calculations include transitions up to J' and J'' equal to 10 for nitrogen and oxygen broadening of $H_2{}^{16}O$, $H_2{}^{18}O$, $H_2{}^{17}O$, $HD^{16}O$, and $D_2{}^{16}O$. The calculations are made with no adjustments of the molecular constants. Initial calculations were made for the isotopomers with the Lennard-Jones (L-J) parameters of hydrogen. The calculations are then repeated with new L-J parameters for H and D [21] and compared with the previous calculations. The half-widths for different isotopomers are compared with those of the principal species and estimating algorithms are discussed. In a companion paper, the half-widths calculated using the L-J parameters for H and D are compared with experimentally determined half-widths.

2. Complex Robert–Bonamy Formalism

2.1. Introduction

The CRB formalism is based on the resolvent operator formalism of Baranger [22], Kolb [23], and Greim [24] (BKG). The application of linked-cluster techniques [25] to the BKG formalism leads to developments [20,26–28] which eliminate the awkward cutoff procedure that characterized earlier theories [29–31]. The formalism is complex valued thus the half-widths and line shifts are obtained from a single calculation. The intermolecular dynamics are treated more realistically than in earlier theories, i.e. using curved rather than straight-line trajectories. This has important consequences in the description of close intermolecular collisions (small impact parameters). Also important for close collision systems is the incorporation in the CRB theory of a short range (L-J 6–12 [32]) atom–atom component to the intermolecular potential. This component has been shown to be essential for a proper description of pressure broadening, especially in systems where electrostatic interactions are weak [33]. (Here, the notion of strong and weak collisions adopts the definition of Oka [34].) The CRB formalism allows the removal of all "adjustable" parameters so as to arrive at a more predictive theory.

The half-width, γ of a ro-vibrational transition f $\leftarrow$ i is given in the CRB formalism by minus the imaginary part of the diagonal elements of the complex relaxation matrix. In computational form, the half-width is usually expressed in terms of the Liouville scattering matrix [22,35]

$$\gamma_{\mathrm{f}\leftarrow\mathrm{i}} = \frac{n_2\bar{v}}{2\pi c}\sum_{J_2}\langle J_2|\rho_2|J_2\rangle\int_0^\infty 2\pi b[1-\cos\{S_1+\mathrm{Im}(S_2)\}\mathrm{e}^{-\mathrm{Re}(S_2)}]\,\mathrm{d}b, \tag{1}$$

where $\bar{v}$ is the mean relative thermal velocity, ρ_2 and n_2 are the density operator and number density of perturbers, and b is the impact parameter. S_1 and S_2 are the first- and second-order terms in the expansion of the Liouville scattering matrix and depend on the intermolecular potential.

In the CRB formalism, the imaginary parts of the S matrix expansion affect the calculation of the half-width. The effect of the imaginary components on the half-widths varies from transition to transition and perturber to perturber but can be as much as 25% [33,36–38]. The change is generally (almost always) in the direction of better agreement with experiment.

2.2. Intermolecular potential

The potential employed in the calculations consists of the leading electrostatic components for the H_2O–X pair (the dipole and quadrupole moments of H_2O with the quadrupole moment of N_2 or O_2), and an atom–atom component [38,39]. The isotropic component of the atom–atom potential is used to define the trajectory of the collision within the semi-classical model of Robert and Bonamy [20].

The atom–atom potential is defined as the sum of pair-wise L-J 6–12 interactions [32] between atoms of the radiating molecule (labeled 1) and the perturbing molecule, N_2 or O_2, (labeled 2),

$$V^{\text{at–at}} = \sum_{i=1}^{n}\sum_{j=1}^{m} 4\varepsilon_{ij}\left\{\frac{\sigma_{ij}^{12}}{r_{1i,2j}^{12}} - \frac{\sigma_{ij}^{6}}{r_{1i,2j}^{6}}\right\}. \tag{2}$$

The subscripts $1i$ and $2j$ refer to the ith atom of molecule 1 and the jth atom of molecule 2, respectively, n and m are the number of atoms in molecules 1 and 2, respectively, and ε_{ij} and σ_{ij} are the L-J parameters for the atomic pairs. The heteronuclear atom–atom parameters can be constructed from homonuclear atom–atom parameters (ε_i and σ_i) by the "combination rules" [40]:

$$\varepsilon_{ij} = \sqrt{\varepsilon_i \varepsilon_j}$$
$$\sigma_{ij} = \frac{\sigma_1 + \sigma_2}{2}. \tag{3}$$

The atom–atom distance, r_{ij} can be expressed in terms of the center of mass separation, R, via the expansion of Sack [41]. Using this fact, Gray and Gubbins [42,43] have shown how the atom–atom potential may be expressed in the form of a spherical tensor expansion,

$$V = \sum_{\substack{\ell_1\ell_2\\ \ell}}\sum_{\substack{n_1\\ m_1m_2\\ m}}\sum_{w,q} \frac{U(\ell_1\ell_2\ell, n_1wq)}{R^{q+\ell_1+\ell_2+2w}} C(\ell_1\ell_2\ell, m_1m_2m) D^{\ell_1}_{m_1n_1}(\Omega_1) D^{\ell_2}_{m_20}(\Omega_2) Y_{\ell m}(\omega), \tag{4}$$

where $C(\ell_1\ell_2\ell; m_1m_2m)$ is a Clebsch–Gordan coefficient, $\Omega_1 = (\alpha_1, \beta_1, \gamma_1)$ and $\Omega_2 = (\alpha_2, \beta_2, \gamma_2)$ are the Euler angles describing the molecular fixed axis relative to the space fixed axis. Subscripts 1 and 2 refer to the radiating molecule (H_2O) and perturbing molecule (N_2 or O_2), respectively, and $\omega = (\theta, \phi)$ describes the relative orientation of the centers of mass. The powers w and q (integers) depend upon the interaction assumed, and the coefficients $U(\ldots)$ are given in Refs. [36,42]. Since the expansion in $(1/R)$ must be truncated, sufficient order must be chosen to insure the convergence of calculated half-widths and line shifts. The order of the expansion has been discussed by Labani et al. [44] and Gamache et al. [38,39,45]. Here the formulation of Neshyba and Gamache [39] expanded to eighth order is used.

2.3. Details of CRB theory

The expressions for the S_1 and S_2 terms in the CRB formalism are described in detail in Refs. [45,46]. Here, only the salient features are summarized. The first-order (imaginary) term, S_1, is

zero for pure rotational transitions so it plays no role in these calculations. The second-order terms are comprised of two basic parts; one describing the internal states of the radiating and perturbing molecules and another describing the interaction and dynamics of the collision. In order to calculate these terms, a number of molecular constants describing the colliding pair are needed.

The second-order term is the complex analog of that appearing in the familiar ATC theory [29–31],

$$S_2 = S^*_{2,i_2} + S_{2,\mathrm{f}_2} + S_{2,\mathrm{middle}}, \tag{5}$$

where the notation is that of Anderson [29]. The case in which the imaginary part of S_2 is ignored has been discussed thoroughly in the literature [30,31,47,48]. Note that $S_{2,\mathrm{middle}}$ has only a real component. The other terms are complex functions and can be written in the form

$$S_{2,\mathrm{f}_2} = \frac{1}{\hbar^2[J_\mathrm{f}][J_2]} \sum_{\substack{\ell_1\ell_2 \\ J_{2'}J_{\mathrm{f}'}}} \sum_{\mathbf{n}^a\mathbf{n}^b} D(\ell_1\ell_2, \mathbf{n}^a\mathbf{n}^b, J_\mathrm{f}J_{\mathrm{f}'}, J_2J_{2'}) F^{\ell_1\ell_2}_{\mathbf{n}^a\mathbf{n}^b}(\omega_{\mathrm{f}_2\mathrm{f}_{2'}}) \tag{6}$$

where $[J] = 2J + 1$, $\mathbf{n} = (n_1, n_2)$ and $\omega_{\mathrm{f}_2,\mathrm{f}_{2'}} = (E_{\mathrm{f}'} - E_\mathrm{f} + E_{2'} - E_2)$ with E_s being the energy of the state f′, f, 2′, or 2. S_{2,i_2} is obtained from Eq. (6) by replacing f with i. The D terms are reduced matrix elements for the internal states of the radiator and perturber [33] and the F terms are the resonance functions for the real and imaginary terms [36] for the potential discussed above.

3. Calculations

All transitions in the rotation band of the principal isotopomer of water vapor were extracted from the HTRAN96 database. From this set all transitions with J'' and J' less than or equal to 10 were retained. This gave 568 transitions. The reason for this choice is that some sets of Watson constants were determined only for transitions up to these rotational quantum number values. Practice has shown that extrapolating the energies and wavefunctions beyond this limit leads to poor results. From this file the rotational quantum numbers were extracted and used as input to the CRB codes. The CRB calculations were made for these transitions for $H_2{}^{16}O$, $H_2{}^{18}O$, $H_2{}^{17}O$, $HD^{16}O$, and $D_2{}^{16}O$ at a temperature of 296 K with nitrogen and oxygen as the perturbing gases.

All molecular parameters used in the calculations are the best available values from the literature. No molecular constants were adjusted to give better agreement with experiment. The dipole and quadrupole moments of water vapor are taken from Refs. [49,50], respectively. The quadrupole moment of nitrogen is from Mulder et al. [51] and that for oxygen is from Stogryn and Stogryn [52]. The numerical values are listed in Table 1. For the principal isotopic species, the heteronuclear atom–atom parameters used are derived from homonuclear–atom–atom parameters obtained by Bouanich [53] using the combination rules [40], and are displayed in Table 2. Until recently atom–atom parameters were not available for the lesser isotopic species: D, ^{18}O and ^{17}O. Recent work has provided a set of atom–atom parameters for D_2 [21] from which the D-N and D-O parameters can be obtained using the combination rules. These values are listed in Table 2. We know of no such data for ^{18}O and ^{17}O, however because of the relatively small mass change it is expected that the atom–atom parameters for ^{16}O are appropriate. Previous CRB calculations that employed atom–atom parameters [54] of H and ^{16}O are compared with the new calculations.

Table 1
Values of electrostatic moments for the water vapor, N_2, and O_2

Molecule	Multipole moment (esu)	Reference
H_2O	$\mu = 1.8549 \times 10^{-18}$	[49]
	$Q_{xx} = -0.13 \times 10^{-26}$	[50]
	$Q_{yy} = -2.5 \times 10^{-26}$	[50]
	$Q_{zz} = 2.63 \times 10^{-26}$	[50]
N_2	$Q_{zz} = -1.4 \times 10^{-26}$	[51]
O_2	$Q_{zz} = -0.4 \times 10^{-26}$	[52]

Table 2
Values of the heteronuclear atom–atom Lennard-Jones (6–12) parameters for the collision pairs considered in this work

Atomic pair	σ/Å	ε/k_B (K)
H–N	2.990	20.46
H–O	2.850	24.13
D–N	2.979	18.49
D–O	2.836	21.81
O–N	3.148	43.90
O–O	3.010	51.73

In the parabolic approximation, the isotropic part of the interaction potential is taken into account in determining the distance, effective velocity, and force at closest approach [20]. To simplify the trajectory calculations, the isotropic part of the atom–atom expansion is fit to an isotropic L-J 6–12 potential.

Finally, the ionization potential of water is taken to be a vibrationally independent 12.6 eV [55]. The polarizability of nitrogen and oxygen are taken from Ref. [56] and are 17.4×10^{-25} and 15.8×10^{-25} cm^3, respectively. The ionization potential of nitrogen is 15.576 eV [57] and the value for oxygen is 12.063 eV [55].

The terms $D(\ldots)$ in Eq. (6) are reduced matrix elements for the internal states of the radiator and perturber. For water vapor, these are evaluated using wavefunctions determined by diagonalizing the Watson Hamiltonian [58] in a symmetric top basis for the vibrational states involved in the transition. For the ground state of $H_2{}^{16}O$ the Watson constants derived by Flaud and Camy-Peyret [59] are used. For $H_2{}^{18}O$ and $H_2{}^{17}O$ the Watson constants of Toth [60] are used. For HDO and D_2O the Watson constants are those of Toth [61]. The rotational constants for N_2 and O_2 are 2.0069 and 1.4377 cm^{-1}, respectively [62].

4. Results

The half-widths at 296 K for all $J \leqslant 10$ transitions in the pure rotation band of $H_2{}^{16}O$, $H_2{}^{18}O$, $H_2{}^{17}O$, $HD^{16}O$, and $D_2{}^{16}O$ were calculated in this study. Excerpts of the full lists are given in

Table 3
N_2-broadened half-widths in units of cm^{-1} atm^{-1} at 296 K for pure rotational transitions of $H_2{}^{16}O$, $H_2{}^{18}O$, $H_2{}^{17}O$, $HD^{16}O$, and $D_2{}^{16}O$

J'	Ka′	Kc′	J''	Ka″	Kc″	$H_2{}^{16}O$	$H_2{}^{18}O$	$H_2{}^{17}O$	HDO	D_2O
6	1	6	5	2	3	0.10210	0.09994	0.10105	0.10448	0.11151
3	1	3	2	2	0	0.11178	0.10934	0.11051	0.10967	0.11427
10	2	9	9	3	6	0.08544	0.08332	0.08343	0.09268	0.10265
5	1	5	4	2	2	0.10537	0.10313	0.10423	0.10584	0.11292
4	1	4	3	2	1	0.10837	0.10605	0.10717	0.10738	0.11337
7	5	3	6	6	0	0.06361	0.06292	0.06350	0.06731	0.08616
6	4	3	5	5	0	0.07507	0.07405	0.07462	0.07743	0.09470
7	5	2	6	6	1	0.06433	0.06372	0.06432	0.06737	0.08630
4	2	3	3	3	0	0.09876	0.09681	0.09777	0.09985	0.11016
6	4	2	5	5	1	0.07794	0.07710	0.07761	0.07761	0.09504
5	3	3	4	4	0	0.08676	0.08530	0.08601	0.08796	0.10329
6	2	4	7	1	7	0.09759	0.09537	0.09655	0.10228	0.10947
8	6	3	7	7	0	0.05405	0.05350	0.05445	0.05943	0.07772
8	6	2	7	7	1	0.05416	0.05363	0.05460	0.05943	0.07775
1	1	0	1	0	1	0.12134	0.11863	0.11992	0.11894	0.12367
5	3	2	4	4	1	0.09091	0.08936	0.09014	0.08956	0.10343
9	7	3	8	8	0	0.04714	0.04654	0.04815	0.05310	0.06947
9	7	2	8	8	1	0.04716	0.04656	0.04819	0.05310	0.06948
2	1	1	2	0	2	0.11540	0.11240	0.11383	0.11670	0.12282
10	8	3	9	9	0	0.04161	0.04105	0.04407	0.04830	0.06175
10	8	2	9	9	1	0.04161	0.04105	0.04409	0.04830	0.06175
9	2	8	8	3	5	0.09056	0.08882	0.08977	0.09321	0.10435
4	2	2	3	3	1	0.10035	0.09820	0.09923	0.10019	0.11195
5	2	4	4	3	1	0.09597	0.09424	0.09510	0.09842	0.10905
2	0	2	1	1	1	0.11471	0.11175	0.11316	0.11654	0.12206
3	1	2	3	0	3	0.11047	0.10776	0.10906	0.11103	0.11804
9	5	5	10	2	8	0.06997	0.06859	0.06706	0.08655	0.09816
1	1	1	0	0	0	0.11410	0.11115	0.11256	0.11408	0.12234
7	2	5	8	1	8	0.09077	0.08868	0.08969	0.10018	0.10765
3	1	2	2	2	1	0.10859	0.10605	0.10726	0.10972	0.11726
6	3	4	5	4	1	0.08321	0.08184	0.08252	0.08732	0.10315
3	2	1	3	1	2	0.10713	0.10454	0.10579	0.10759	0.11708
8	5	4	7	6	1	0.05942	0.05877	0.05960	0.06613	0.08715
7	4	4	6	5	1	0.07137	0.07051	0.07099	0.07624	0.09543
8	5	3	7	6	2	0.06194	0.06161	0.06259	0.06619	0.08754
4	2	2	4	1	3	0.10677	0.10435	0.10550	0.10481	0.11432
9	6	4	8	7	1	0.04997	0.04937	0.05130	0.05734	0.07876

Table 3 for N_2-broadening and in Table 4 for O_2-broadening. Electronic copies of the complete tables can be obtained from one of the authors (RRG).

With new atom–atom parameters available for D_2 the heteronuclear atom–atom parameters for D-N and D-O can be derived. These are listed in Table 2. The use of these constants in place of the H-N and H-O constants leads to different half-widths for HDO and D_2O. For HDO-N_2 the

Table 4
O_2-broadened half-widths in units of cm^{-1} atm^{-1} at 296 K for pure rotational transitions of $H_2{}^{16}O$, $H_2{}^{18}O$, $H_2{}^{17}O$, $HD^{16}O$, and $D_2{}^{16}O$

J'	Ka′	Kc′	J''	Ka″	Kc″	$H_2{}^{16}O$	$H_2{}^{18}O$	$H_2{}^{17}O$	HDO	D_2O
6	1	6	5	2	3	0.05401	0.05292	0.05335	0.05401	0.06078
3	1	3	2	2	0	0.06234	0.06098	0.06158	0.05919	0.06575
10	2	9	9	3	6	0.04669	0.04583	0.04594	0.04607	0.05254
5	1	5	4	2	2	0.05643	0.05524	0.05572	0.05553	0.06241
4	1	4	3	2	1	0.05918	0.05792	0.05845	0.05715	0.06389
7	5	3	6	6	0	0.04223	0.04109	0.04172	0.04148	0.04821
6	4	3	5	5	0	0.04569	0.04449	0.04511	0.04449	0.05171
7	5	2	6	6	1	0.04231	0.04120	0.04183	0.04148	0.04824
4	2	3	3	3	0	0.05490	0.05361	0.05422	0.05301	0.06084
6	4	2	5	5	1	0.04612	0.04498	0.04557	0.04454	0.05179
5	3	3	4	4	0	0.04983	0.04858	0.04920	0.04804	0.05593
6	2	4	7	1	7	0.05190	0.05089	0.05128	0.05223	0.05881
8	6	3	7	7	0	0.03938	0.03829	0.03899	0.03909	0.04515
8	6	2	7	7	1	0.03939	0.03830	0.03901	0.03909	0.04515
1	1	0	1	0	1	0.06713	0.06601	0.06637	0.06494	0.06896
5	3	2	4	4	1	0.05065	0.04944	0.05003	0.04848	0.05601
9	7	3	8	8	0	0.03695	0.03594	0.03670	0.03713	0.04245
9	7	2	8	8	1	0.03696	0.03594	0.03671	0.03713	0.04245
2	1	1	2	0	2	0.06513	0.06373	0.06429	0.06415	0.06912
10	8	3	9	9	0	0.03435	0.03337	0.03463	0.03554	0.04003
10	8	2	9	9	1	0.03435	0.03337	0.03464	0.03554	0.04003
9	2	8	8	3	5	0.04782	0.04702	0.04735	0.04654	0.05388
4	2	2	3	3	1	0.05515	0.05381	0.05443	0.05309	0.06141
5	2	4	4	3	1	0.05224	0.05102	0.05157	0.05177	0.05937
2	0	2	1	1	1	0.06518	0.06366	0.06431	0.06442	0.06935
3	1	2	3	0	3	0.06044	0.05910	0.05964	0.06056	0.06666
9	5	5	10	2	8	0.04113	0.04011	0.04048	0.04446	0.05042
1	1	1	0	0	0	0.06504	0.06347	0.06414	0.06401	0.07056
7	2	5	8	1	8	0.04958	0.04856	0.04892	0.05065	0.05689
3	1	2	2	2	1	0.05989	0.05846	0.05911	0.05887	0.06608
6	3	4	5	4	1	0.04740	0.04624	0.04678	0.04712	0.05533
3	2	1	3	1	2	0.05893	0.05758	0.05816	0.05783	0.06576
8	5	4	7	6	1	0.03981	0.03872	0.03939	0.04024	0.04838
7	4	4	6	5	1	0.04330	0.04218	0.04274	0.04320	0.05170
8	5	3	7	6	2	0.04016	0.03915	0.03982	0.04026	0.04846
4	2	2	4	1	3	0.05693	0.05574	0.05620	0.05570	0.06372
9	6	4	8	7	1	0.03702	0.03599	0.03686	0.03789	0.04529

change of constants resulted in all half-widths being smaller than the previously calculated values. The average change was −4.6% with a maximum change of −7.4%. This is shown in Fig. 1. This improves the comparison with experiment. For HDO-O_2 the change to the deuterium parameters reduces all the half-widths, see Fig. 2, with the average change being −8.6%. The smallest decrease is 5.8% and the largest 11.7%. This leads to much better agreement with measurement. For

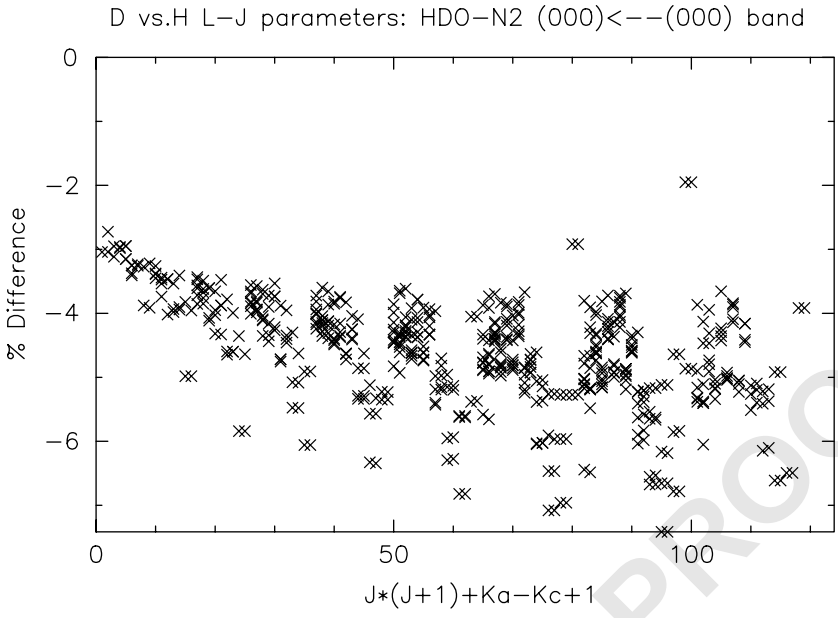

Fig. 1. Percent difference half-widths calculated using L-J parameters for D minus half-widths calculated using L-J parameters for H; HDO-N_2 (000)-(000) band.

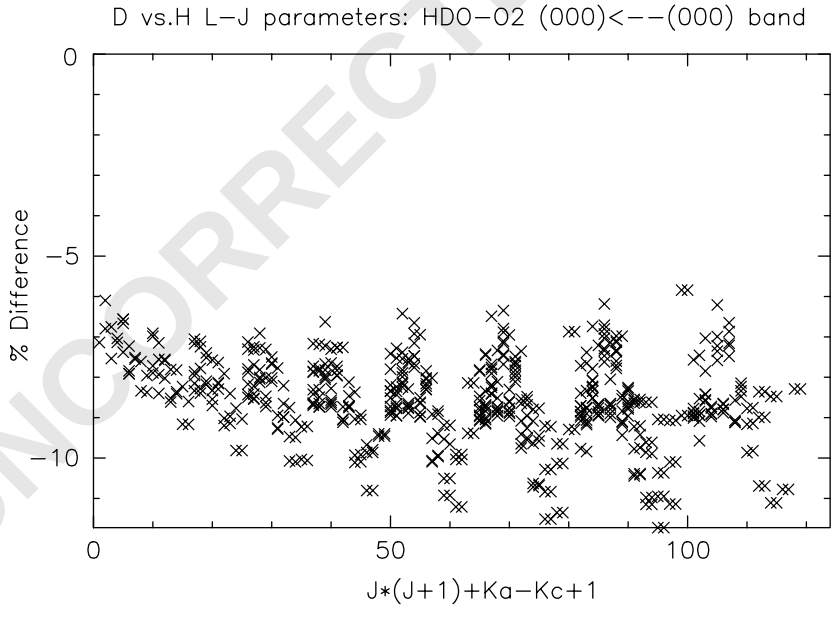

Fig. 2. Percent difference half-widths calculated using L-J parameters for D minus half-widths calculated using L-J parameters for H; HDO-O_2 (000)-(000) band.

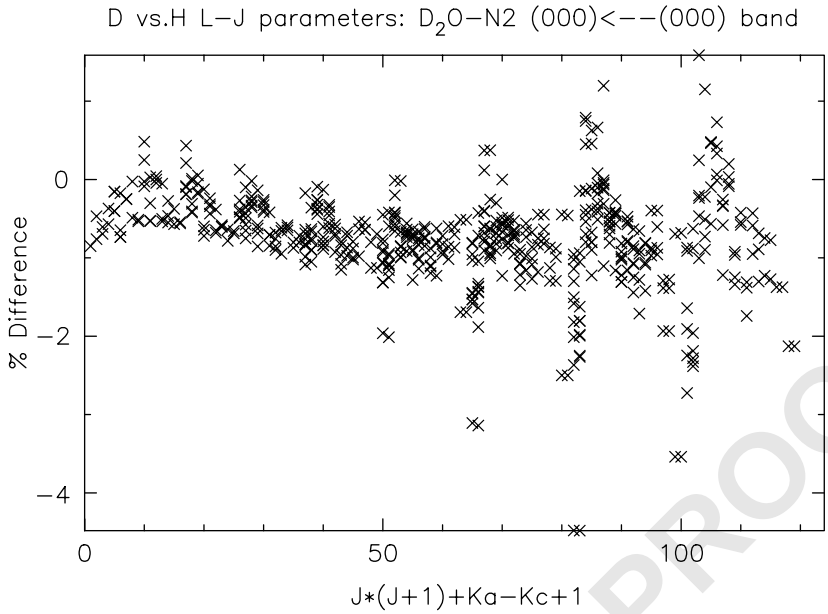

Fig. 3. Percent difference half-widths calculated using L-J parameters for D minus half-widths calculated using L-J parameters for H; D_2O-N_2 (000)-(000) band.

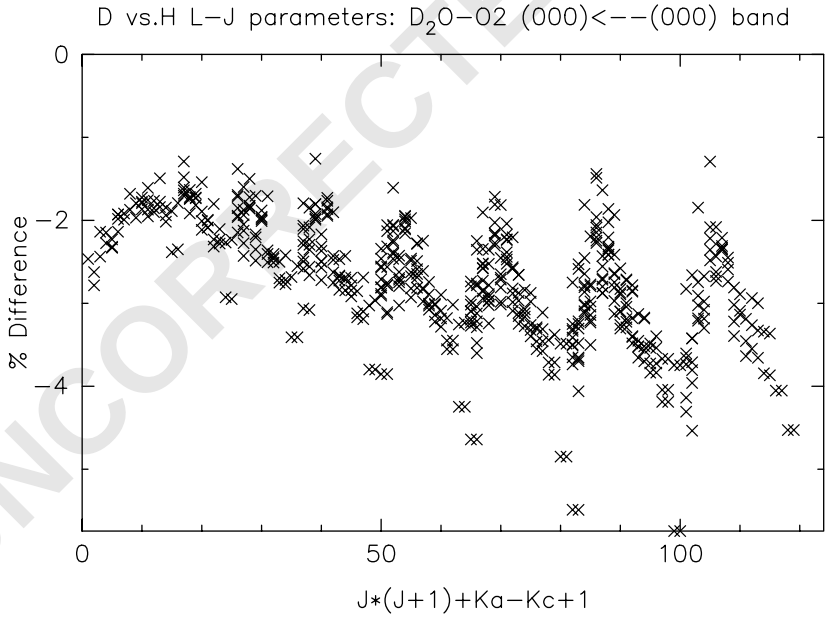

Fig. 4. Percent difference half-widths calculated using L-J parameters for D minus half-widths calculated using L-J parameters for H; D_2O-O_2 (000)-(000) band.

Table 5
Max, Min, and average ratios and standard deviation of $H_2{}^{16}O$ half-widths divided by half-width of less abundant isotopomer for N_2-broadening

N_2-broadening	$H_2{}^{18}O$	$H_2{}^{17}O$	HDO	D_2O
Max ratio	1.048	1.080	1.100	0.992
Min ratio	0.994	0.858	0.567	0.420
Average % difference	1.018	1.000	0.919	0.786
Standard deviation	0.007	0.026	0.103	0.128

Columns are labeled by lesser abundant isotopomer.

Table 6
Max, Min, and average ratios and standard deviation of $H_2{}^{16}O$ half-widths divided by half-width of less abundant isotopomer for O_2-broadening

O_2-broadening	$H_2{}^{18}O$	$H_2{}^{17}O$	HDO	D_2O
Max ratio	1.055	1.046	1.105	0.990
Min ratio	1.011	0.955	0.641	0.544
Average % difference	1.024	1.009	0.994	0.862
Standard deviation	0.005	0.009	0.063	0.069

Columns are labeled by lesser abundant isotopomer.

D_2O-N_2 the change of parameters led to a lowering of the half-widths in general, however some increased as much as 1.6%, see Fig. 3. The average change was a lowering of the half-widths by ~0.8%. These changes result in better agreement with measurement. Finally, for D_2O-O_2, the change lowered all the half-widths by 2.7% on average with a max lowering of 5.8%, see Fig. 4. Again, this leads to better agreement with experiment but the overall agreement for this system is still in question.

The study now focuses on the change in the half-width as a function of isotopomer. Ratios of the half-widths of the principal isotopomer divided by the half-width of the lesser abundant isotopomers for the same rotational transitions were determined. The minimum and maximum ratio, the average ratio and the standard deviation of the distribution are presented in Table 5 for N_2-broadening and in Table 6 for O_2-broadening. In Fig. 5 the ratios are plotted for N_2-broadening and in Fig. 6 for O_2-broadening. The open circles are for the ratio $\gamma(H_2{}^{16}O)/\gamma(H_2{}^{18}O)$, the solid triangles are for the ratio $\gamma(H_2{}^{16}O)/\gamma(H_2{}^{17}O)$, the x symbols are for the ratio $\gamma(H_2{}^{16}O)/\gamma(HD^{16}O)$, and the open squares are for the ratio $\gamma(H_2{}^{16}O)/\gamma(D_2{}^{16}O)$. As might be expected, the water vapor species with the lesser abundant oxygen isotopes, ^{18}O and ^{17}O, do not show great differences from the $H_2{}^{16}O$ half-widths. Caution should be exercised in interpreting these results since the atom–atom parameters employed are those of ^{16}O. The average ratios for $H_2{}^{18}O$ are 1.018 and 1.024 for N_2- and O_2-broadening, respectively, with little spread. For $H_2{}^{17}O$ the average ratios are 1.000 and 1.009 for N_2- and O_2-broadening, respectively, and the spread around these values is somewhat larger than that for $H_2{}^{18}O$ but still not great.

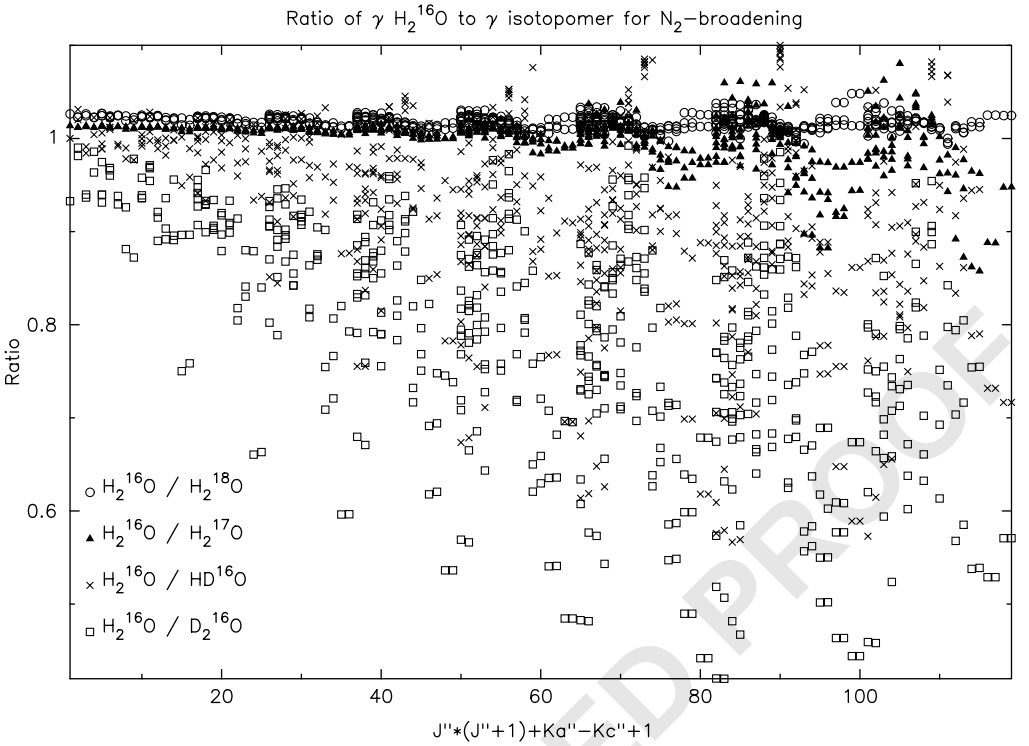

Fig. 5. Ratio of $\gamma(H_2{}^{16}O)$ over γ (lesser abundant isotopomers) for N_2-broadening of 568 (000)-(000) band transitions; open circle symbols are ratios to $H_2{}^{18}O$, solid triangle symbols are ratios to $H_2{}^{17}O$, x symbols are ratios to HDO, and open square symbols are ratios to D_2O.

For HDO the spread in the ratios is large. For N_2-broadening the average ratio is 0.929 but the max and min ratios are 1.100 and 0.567, respectively. For O_2-broadening the results are similar with the average ratio equal to 0.994 and max and min values of 1.105 and 0.641, respectively. For D_2O the spread in the ratios increases. The average ratio for N_2-broadening is 0.786 and for O_2-broadening 0.862. The max ratios are 0.992 and 0.990 and the min ratios are 0.420 and 0.544 for N_2- and O_2-broadening, respectively.

The current algorithm for water vapor used in HITRAN simply adds a half-width to a line based on the rotational quantum numbers of the transition. Vibrational dependence is ignored as is the particular isotopic species in question. Ignoring the question of the accuracy of the half-widths of the principal species in the database, the added error from using the half-width of the principal species for one of the lesser abundant species can be addressed. The above analysis suggests that for the $H_2{}^{18}O$ isotopomer this procedure will add an additional 2% error. For $H_2{}^{17}O$ the additional error can be as large as 15% for N_2-broadening and about 5% for O_2-broadening. For the deuterated species the error increases. For HDO the errors are as large as 38% and 36% for N_2- and O_2-broadening, respectively. For D_2O, which is currently not on the HITRAN database, the errors from this procedure are 47% and 37% for N_2- and O_2-broadening, respectively.

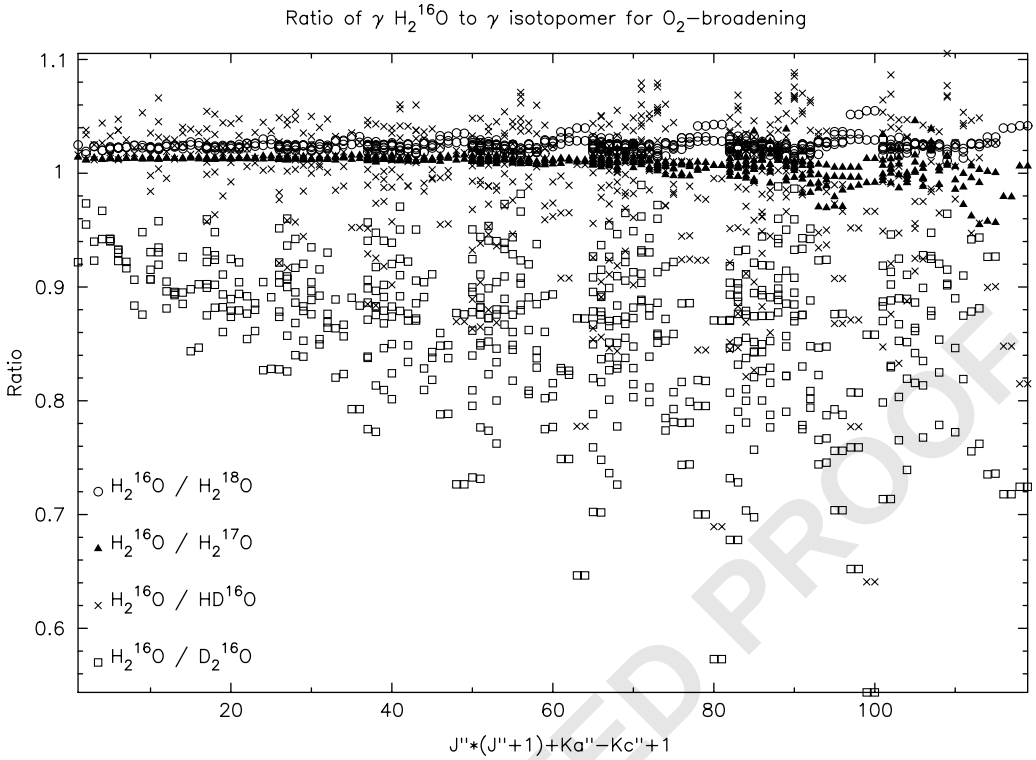

Fig. 6. Ratio of $\gamma(H_2{}^{16}O)$ over γ (lesser abundant isotopomers) for O_2-broadening of 568 (000)-(000) band transitions; open circle symbols are ratios to $H_2{}^{18}O$, solid triangle symbols are ratios to $H_2{}^{17}O$, x symbols are ratios to HDO, and open square symbols are ratios to D_2O.

5. Summary

Half-widths have been determined via CRB theory for five isotopomers of water vapor; $H_2{}^{16}O$, $H_2{}^{18}O$, $H_2{}^{17}O$, $HD^{16}O$, and $D_2{}^{16}O$. The calculations were made at 296 K for nitrogen and oxygen as broadening gases and limited to rotational transitions with J'' and J' less than or equal to 10. When appropriate, the potential employed L-J parameters for the D-N and D-O interactions, which were obtained using the combination rules and newly determined D_2 L-J parameters. These calculations were compared with previous calculations made using only hydrogen L-J parameters and it is observed that the half-widths calculated in this study for the deuterated species of water vapor are in better agreement with measured values.

For each rotational transition studied, ratios of the half-width of $H_2{}^{16}O$ to the lesser abundant isotopomers were determined. It is observed that for the non-deuterated species, the differences between the principal isotopomer half-width and that of the lesser abundant species is small. However, for the deuterated species these differences are large. The errors introduced by algorithms using the half-width of $H_2{}^{16}O$ for the other species, such as that used by HITRAN, are estimated.

The calculations for the $H_2{}^{18}O$ and $H_2{}^{17}O$ isotopomers use the L-J parameters for $^{16}O_2$ to determine the heteronuclear L-J parameters. While it is not expected to be a large difference it would be interesting to obtain L-J parameters for $^{18}O_2$ and $^{17}O_2$ to confirm this assumption.

It is observed that relatively small changes in the atom–atom parameters in going from H to D, roughly 10% for the σ and 0.5% for the ε values, lead to noticeable changes in the calculated half-widths. It should be realized that the combination rule algorithm must be questioned. If possible, atom–atom parameters should be adjusted around the current values based on experiment.

Finally, the ratios and error analyses are based on the calculated half-widths and do not question the accuracy of the calculated values. The comparison of the CRB calculated values with the available measurements will be done in an accompanying paper.

Acknowledgements

The authors are pleased to acknowledge support of this research by the National Science Foundation through Grant No. ATM-9415454. Any opinions, findings, and conclusions or recommendations expressed in this material are those of the author(s) and do not necessarily reflect the views of the National Science Foundation.

References

[1] Hartmann DL. Global physical climatology. Boston: Academic Press, Inc, 1994.
[2] Rothman LS, Rinsland CP, Goldman A, Massie ST, Edwards DP, Flaud J-M, Perrin A, Dana V, Mandin J-Y, Schroeder J, McCann A, Gamache RR, Wattson RB, Yoshino K, Chance KV, Jucks KW, Brown LR, Nemtchinov V, Varanasi P. The HITRAN molecular spectroscopic database and hawks (HITRAN atmospheric workstation): 1996 edition. JQSRT 1998;60:665–710.
[3] Jacquinet-Husson N, Arié E, Ballard J, Barbe A, Bjoraker G, Bonnet B, Brown LR, Camy-Peyret C, Champion J-P, Chédin A, Chursin A, C1erbaux C, Duxbury G, Flaud J-M, Fourrié N, Fayt A, Graner G, Gamache RR, Goldman A, Go1ovko Vl, Guelachvili G, Hartmann J-M, Hilico JC, Hillman J, Lefèvre G, Lellouch E, Mikhailenko SN, Naumenko OV, Nemtchinov V, Newnham DA, Nikitin A, Orphal J, Perrin A, Reuter DC, Rinsland CP, Rosenmann L, Rothman LS, Scott NA, Selby J, Sinitsa LN, Sirota JM, Smith MAH, Smith KM, Tyuterev VlG, Tipping RH, Urban S, Varanasi P, Weber M. The 1997 spectroscopic GEISA databank. JQSRT 1999;62:205–54.
[4] Gamache RR, Davies RW. Theoretical calculations of molecular nitrogen-broadened halfwidths of water using quantum Fourier transform theory. Appl Opt 1983;22:4013–9.
[5] Davies RW. Optimum Combination Algorithm. private communication, University of Massachusetts Lowell, 1982.
[6] Gamache RR, Hartmann JM, Rosenmann L. Collisional broadening of water-vapor lines: I. A survey of experimental results. JQSRT 1994;52:481–99.
[7] Smith MAH, Gordley LL. Sensitivity of ozone retrievals in limb-viewing experiments to errors in line-width parameters. JQSRT 1983;29:413–8.
[8] Chu WP, Chiou EW, Larsen JC, Thomason LW, Rind D, Buglia JJ, Oltmans S, McCormick MP, McMaster LM. Algorithms and sensitivity analyses for Stratospheric Aerosol and Gas Experiment II water vapor retrieval. J Geophys Res 1993;98:4857–66.
[9] Proceedings, National Aeronautics and Space Administration Workshop on Spectral Line Parameters, NASA Langley Research Center, Hampton, VA, 1992.
[10] Atmospheric Spectroscopy Applications Workshop, ASA REIMS 96, Université de Reims, Champagne Ardenne, September 4–6, 1996.
[11] Margolis J. NASA private communication, 1998.
[12] Pumphrey H, Bühler S. Instrumental and spectral parameters: their effect on and measurement by microwave limb sounding of the atmosphere. JQSRT 2000;64:421–37.
[13] Devi VM, Rinsland CP, Benner DC, Smith MAH. Tunable diode laser measurements of air and N2 broadened half-widths in the ν_2 band of D_2O. Appl Opt 1986;25:336.

[14] Devi VM, Benner DC, Rinsland CP, Smith MAH, Barry DS. Diode laser measurements of air and nitrogen broadening in the $\nu 2$ bands of HDO, $H_2{}^{16}O$ and $H_2{}^{18}O$. J Mol Spec 1986;117:403–7.
[15] Rinsland CP, Smith MAH, Devi VM, Benner DC. Measurements of Lorentz-broadening coefficients and pressure-induced line shift coefficients in the $\nu 2$ band of D216O. J Mol Spec 1991;150:173–83.
[16] Smith MAH, Rinsland CP, Devi VM, Benner DC. Measurements of Lorentz-broadening coefficients and pressure induced line shift coefficients in the $\nu 2$ band of HD16O. J Mol Spec 1991;150:640–6.
[17] Toth RA. Air and N2 broadening parameters of HDO and D2O; 709 to 1936 cm^{-1}. J Mol Spec 1999;198:358–70.
[18] Toth RA. Air- and N_2-broadening parameters of water vapor: 604 to 2271 cm^{-1}. J Mol Spec 2000;201:218–43.
[19] Levy A, Lacome N, Chackerian Jr. C. In: Rao KN, Weber A, editors. Spectroscopy of the Earth's atmosphere and interstellar molecules. Boston: Academic Press, Inc, 1992.
[20] Robert D, Bonamy J. Short range force effects in semiclassical molecular line broadening calculations. J Phys 1979;40:923–43.
[21] Wang WF. Atomic-potential parameters for H2 and D2: quantum corrections in the calculation of second virial coefficients. JQSRT, 2002, in press.
[22] Baranger M. General impact theory of pressure broadening. Phys Rev 1958;112:855–65.
[23] Kolb AC, Griem HR. Theory of line broadening in multiplet spectra. Phys Rev 1958;111:514–21.
[24] Griem H. Plasma spectroscopy. New York: McGraw Hill, 1964.
[25] Kubo R. J Phys Soc Japan 1962;17:1100–20.
[26] Korff D, Leavitt RP. Calculation of impact broadened half width parameters for hydrogen chloride using a natural cutoff theory. Phys Lett A 1975;53:351.
[27] Leavitt RP, Korff D. Cutoff-free theory of impact broadening and shifting in microwave and infrared spectra. J Chem Phys 1981;74:2180–8.
[28] Looney JP, Herman RM. Air broadening of the hydrogen halides-I. Nitrogen-broadening and shifting in the hydrogen chloride fundamental. JQSRT 1987;37:547–57.
[29] Anderson PW. Dissertation, Harvard University, 1949.
[30] Anderson PW. Phys Rev 1949;76:647–61;
Anderson PW. Phys Rev 1950;80:511–3.
[31] Tsao CJ, Curnutte Jr. B. JQSRT 1962;2:41–91.
[32] Lennard-Jones JE. Proc Roy Soc 1924;A 106:463–77.
[33] Neshyba SP, Lynch R, Gamache RR, Gabard T, Champion J-P. Pressure-induced widths and shifts for the $\nu 3$ band of methane. J Chem Phys 1994;101:9412–21.
[34] Oka T. In: Bates DR, editor. Advances in atomic and molecular physics. New York: Academic Press, 1973.
[35] Ben-Reuven A. Spectral line shapes in gases in the binary-collision approximation, In: Prigogine I, Rice SA, editors. Advances in chemistry and physics, vol. 20. New York: Academic Press, 1975. p. 235.
[36] Lynch R, Gamache RR, Neshyba SP. Fully complex implementation of the Robert–Bonamy formalism: half widths and line shifts of H2O broadened by N2. J Chem Phys 1996;105:5711–21.
[37] Gamache RR, Lynch R, Plateaux JJ, Barbe A. Halfwidths and line shifts of water vapor broadened by CO_2: measurements and complex Robert–Bonamy formalism calculations. JQSRT 1997;57:485–96.
[38] Gamache RR, Lynch R, Neshyba SP. New developments in the theory of pressure-broadening and pressure-shifting of spectral lines of H_2O: the complex Robert–Bonamy formalism. JQSRT 1998;59:319–35.
[39] Neshyba SP, Gamache RR. Improved line-broadening coefficients for asymmetric rotor molecules with application to ozone lines broadened by nitrogen. JQSRT 1993;50:443–53.
[40] Hirschfelder JO, Curtiss CF, Bird RB. Molecular theory of gases and liquids. New York: Wiley, 1964.
[41] Sack RA. J Math Phys 1964;5:260.
[42] Gray CG, Gubbins KE. Theory of molecular fluids. Oxford: Clarendon Press, 1984.
[43] Gray CG. Can J Phys 1968;46:135.
[44] Labani B, Bonamy J, Robert D, Hartmann J-M, Taine J. Collisional broadening of rotation-vibration lines for asymmetric top molecules. I. Theoretical model for both distant and close collisions. J Chem Phys 1986;84: 4256–67.
[45] Lynch R, Gamache RR, Neshyba SP. N_2 and O_2 induced halfwidths and line shifts of water vapor transitions in the $(301) \leftarrow (000)$ and $(221) \leftarrow (000)$ bands. JQSRT 1998;59:595–613.
[46] Lynch R. Ph.D. dissertation, Physics Department, University of Massachusetts Lowell, June 1995.

[47] Yamamoto G, Aoki T. Line broadening theory of asymmetric-top molecule. JQSRT 1972;12:227.
[48] Moazzen-Ahmadi MN, Roberts JA. Linewidth parameters in the rotational spectrum of nitrogen dioxide. J Mol Spec 1982;96:336.
[49] Shostak SL, Muenter JS. The dipole moment of water. II. Analysis of the vibrational dependence of the dipole moment in terms of a dipole moment function. J Chem Phys 1991;94:5883–90.
[50] Flygare WH, Benson RC. Molecular Zeeman effect in diamagnetic molecules and the determination of molecular magnetic moments (g values), magnetic susceptibilities, and molecular quadrupole moments. Mol Phys 1971;20: 225–50.
[51] Mulder F, Van Dijk G, Van der Avoird A. Multipole moments, polarizabilities, and anisotropic long range interaction coefficients for nitrogen. Mol Phys 1980;39:407–25.
[52] Stogryn DE, Stogryn AP. Molecular multipole moments. Mol Phys 1966;11:371–93.
[53] Bouanich J-P. Site–site Lennard-Jones potential parameters for nitrogen, oxygen, hydrogen, carbon monoxide and carbon dioxide. JQSRT 1992;47:243–50.
[54] Gamache RR. Isotopomer dependence of N_2- and O_2-broadened half-widths of water vapor transitions. In: Proceedings of the Sixteenth Colloquium on High Resolution Molecular Spectroscopy, University of Bourgogne, Dijon, 6–10 September, 1999.
[55] Lide DR, editor. CRC handbook of physics and chemistry, 77th ed. Clevland, OH: The Chemical Rubber Company, 1996.
[56] Bogaard MP, Orr BJ. In: Buckingham AD, editor. MPT international review of science, physical chemistry, Molecular structure and properties, Series Two, vol. 2. London: Butterworths, 1975 [chapter 5].
[57] Lofthus A. The molecular spectrum of nitrogen. Department of Physics, University of Oslo, Blindern, Norway, Spectroscopic Report No. 2, 1, 1960.
[58] Watson JKG. Determination of centrifugal distortion coefficients of asymmetric-top molecules. J Chem Phys 1967;46:1935–49.
[59] Flaud J-M, Camy-Peyret C. Private communication, University of Pierre and Marie Curie, Paris, France, 1994.
[60] Toth RA. $HD^{16}O$, $HD^{18}O$, $HD^{17}O$ Transition Frequencies and Strengths in the $\nu 2$ bands. J Mol Spec 1993;162: 20–40.
[61] Toth RA. $D_2{}^{16}O$ and $D_2{}^{18}O$ Transition frequencies and strengths in the $\nu 2$ bands. J Mol Spec 1993;162:41–54.
[62] Huber KP, Herzberg G. Molecular spectra and molecular structure constants of diatomic molecules. New York: Van Nostrand, 1979.